19

Visualization of Sorption Dynamics: Application of Confocal Laser Scanning Microscope Technique

Takashi Hasegawa[1,2], Kiyoshi Matsumoto[3] and Toshiro Matsui[2]
[1]R&D Planning Division, Tobacco Business Headquarters, Japan Tobacco Inc., 2-2-1 Toranomon, Minato-ku, Tokyo 105-8422
[2]Bioscience and Biotechnology, Graduate School of Agriculture, Kyushu University, 6-10-1 Hakozaki, Higashi-ku, Fukuoka 812-8581
[3]Faculty of Biotechnology and Life Science, Department of Applied Microbial Technology, Sojo University, 4-22-1 Ikeda, Kumamoto 860-0082
Japan

1. Introduction

The sorption of compounds such as liquid additives and vapor components into polymer materials is one of the most deteriorative phenomena for polymer products. In the field of material engineering, various additives are used in the process of manufacturing polymer products for the purpose of improving product functions. For example, in the manufacturing process of thermoplastics for plastic lapping and rubber materials, plasticizers are added to increase flexibility, toughness and/or transparency [1, 2]. In those cases, the diffusion of plasticizer in polymer materials is associated with the stability of product quality [3-5]. Food industries aim to avoid the serious deterioration due to the loss of flavors responsible for product quality, through sorption into packaging materials [6-8].
In past decades, numerous studies on sorption behavior of chemicals into polymer materials have been reported, mainly on the basis of their physicochemical properties [3-5, 9, 10]. One perspective is an investigation of diffusion and distribution of plasticizers themselves in polymer materials [3-5], and another is an estimation of the influence of co-existing plasticizers on the sorption behavior of penetrant compounds [9, 10]. In these studies, the sorption amount of penetrant chemicals has been determined by measuring a change in weight and/or by extracting absorbed penetrants with solvents in evaluating the diffusion kinetics of penetrant chemicals. However, no *in situ* examination of penetration or distribution of absorbed chemicals has been performed due to the lack of real-time and non-destructive assays. To overcome these problems, we have clarified the dynamic sorption behavior of flavors into polymer films [11-15]. The physical and chemical parameters of chemicals and/or polymers such as molar volume, free energy, free volume and solubility parameters have been clarified to be characterized as contributors for flavor sorption [11-13] by determining the sorption dynamics with our proposed aqueous and vaporous penetration methods [14, 15]. The proposed convenient penetration methods, however, could not provide any *in situ* information on the real-time sorption behavior of penetrants in polymers.

Although observational methodology using time-of-flight secondary ion mass spectrometry (TOF-SIMS) was applied to obtain the cross-sectional distribution of penetrants in polymer films or fibers [16], destruction treatment of samples was needed to determine the concentration of penetrants in each sectional region.
The lack of non-destructive observational methodology, thus, led us to apply the use of a confocal laser scanning microscope (CLSM) for real-time monitoring of penetrants in polymers.
CLSM has been widely used for observation and/or analysis of mass transfer phenomena in the field of physiology and pharmacology with fluorescent labeling technique or fluorescent reagent mixture [17-23]. In physiology, there has been reports on CLSM usage by researchers for monitoring the formation process of poly(ethylene glycol) micro- and nano-gels [17] or surface cross-linked structure of poly(vinyl alcohol) [18]. In pharmacology, CLSM has been applied to analyze the transport phenomenon of protein [19, 20] or the dynamics of glucose transporter in lipocyte [21].
Recently, the material engineering field has recorded reports on attempts to apply CLSM. For example, there was an observation by CLSM [22] on the absorption behavior of glycerin containing fluorescent dye into the fiber as an analytical method for evaluating the hydrophilicity of the surface of nylon fiber. In addition, to investigate the plasticizing effect of supercritical fluid treatment for polypropylene, the distribution of a fluorescent probe mixed in the film has been analyzed by CLSM [23].
In this chapter, we reviewed the application of CLSM technique to real-time and non-destructive observation of fluorescent reagent sorbed into polymer materials [24-26]. Subsequently, a novel observational methodology for sorption behavior was established by CLSM in section 2. In section 3, effects of various additives on sorption behavior of fluorescent reagent were evaluated. Lastly, effects of film types and film depth on diffusion coefficient of fluorescent reagent were examined as a further development of CLSM methodology in section 4. As a fluorescent reagent and a polymer material, perylene and cellulose acetate (CA) were used, respectively. CA is widely used in various industrial fields such as for cigarette filters, clothing, water purification and medical applications [27, 28], and there are a number of studies reported on the sorption behavior of water and alcohols into CA [29-31]. Additives for dissolving penetrant perylene were glycerol triacetate (GTA), triethylene glycol diacetate (TEGDA), 1,3-butylene glycol diacetate (BGDA), paraffin liquid and polyethylene glycol 200 (PEG), in which GTA, TEGDA and BGDA are known as the plasticizers for CA [32, 33], and paraffin liquid and PEG for additives of CA filters in cigarette industrial field [34, 35].

2. Establishment of CLSM methodology for visualizing sorption behavior

2.1 Fluorescent properties of samples

Closed-system CA film (CCA) for CLSM analysis was prepared according to the following procedure. CA flake with a degree of substitution of 2.5 (Mw = 1.0×10^5 g/mol, Figure 1) and kindly supplied from Daicel Chemical Industries Ltd. (Osaka, Japan) was dissolved in acetone to make a 2.0 w/v % solution without further purification. An aliquot (200 μl) of CA solution was then put into a film-making-unit with a penicillin cup and cover glass as shown in Figure 2. Excess acetone was vaporized at room temperature for 15 h, and the prepared CA film onto the surface of film-making-unit was then dried *in vacuo* overnight. The prepared films were 95 ± 5 μm thick.

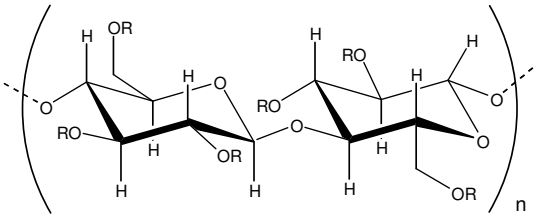

Fig. 1. Chemical structure of CA.

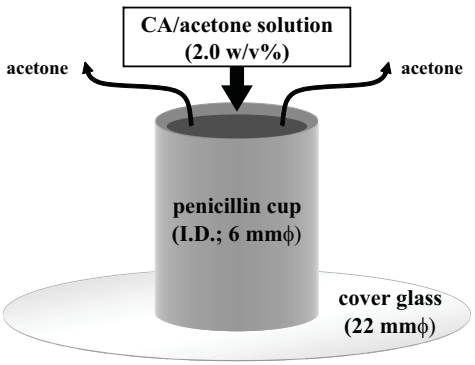

Fig. 2. Preparation of CCA sample on film-making-unit.

And then, perylene (Mw = 252.3 g/mol, λ_{ex} = 411 nm, λ_{em} = 470 nm, Wako Pure Chemical Industries Ltd., Osaka, Japan) and GTA (Mw = 218.2 g/mol, Sigma-Aldrich, Tokyo, Japan) were mixed to make perylene/GTA mixture at room temperature by dissolving perylene in GTA to reach a molar ratio of from 2.2 to 11 × 10^{-5}. The molar ratio of perylene, C_{per}, was defined as formula (1).

$$C_{per}\,[-] = \frac{Perylene\ amount\,[mol]}{Perylene\ amount\,[mol] + GTA\ amount\,[mol]} \tag{1}$$

To evaluate fluorescent properties of CCA sample, GTA and perylene/GTA mixture, the fluorescent spectra were obtained by a CLSM system (CLSM system A1, Nikon Corporation, Tokyo, Japan) equipped with a dry objective lens (CFI Plan Apo VC 20×, Nikon Corporation, Tokyo, Japan). The spectrum of CCA sample was obtained by placing a film sample on a microscope directly, while the spectra of GTA and perylene/GTA mixture were obtained by pipetting 4 μl of the solution onto a cover glass placed on a microscope. A diode laser (408 nm, 290-330 μW) was used as an excitation laser, and the fluorescence excited from the around cover glass surface was detected. Figure 3 shows the fluorescent spectra of CCA sample, GTA and perylene/GTA mixture when excited by a diode laser at 408 nm. The spectra clearly demonstrate that only perylene/GTA mixture had significant perylene-induced fluorescent intensity, indicating that any interfering fluorescences may be excluded to investigate the distribution dynamics of penetrant, perylene.

Fluorescent intensity of perylene/GTA mixture was measured by the above-mentioned CLSM conditions at room temperature. The intensity of reflected fluorescence in the range

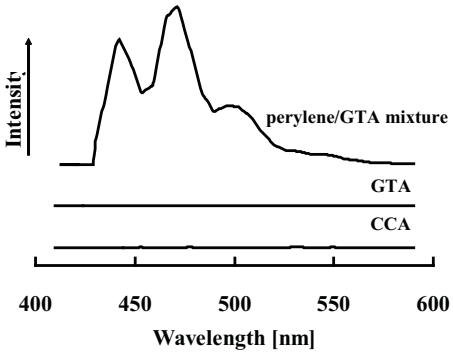

Fig. 3. Fluorescent spectra of CCA sample, GTA and perylene/GTA mixture.

of 450 ± 25 nm of wavelength was measured from confocal images around the cover glasses surface by using an optical filter. Figure 4 shows the relationship between the C_{per} and fluorescent intensity in each mixture. Three replicates of CLSM analysis of perylene (± standard deviation, SD) were performed for this study. As a result, the fluorescent intensity presented a good linearity (r = 0.998) with C_{per} ranging from 2.2 to 11 × 10^{-5}.

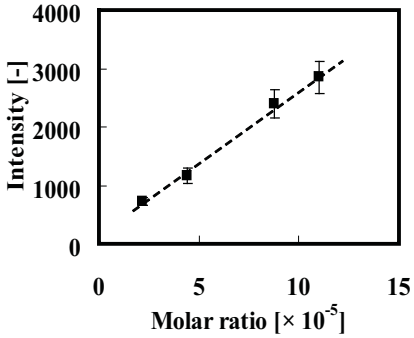

Fig. 4. Relationship between molar ratio of perylene and fluorescent intensity.

2.2 Effect of CLSM conditions on visualized sorption behavior

Perylene in CCA sample was observed by CLSM at several analytical conditions. That is, the fluorescent intensity of distributed perylene in CCA sample was measured as follows. Prior to perylene measurement by CLSM, the air-contact surface of the CCA sample was determined by transmission image using a halogen lump. Then, CLSM analysis was carried out at 60 min after placing 4 μl of perylene/GTA mixture onto CCA sample. Confocal images were obtained by scanning the diode laser in the cross-sectional region of the CCA sample with intervals along the Z-axis (Figure 5); the depth from the air-contact surface of the CCA sample were ± 10 or ± 30 μm with intervals at 1 or 3 μm, respectively. The confocal imaging area was approximately 640 × 640 μm on the X-Y surface, and both low- (scanning speed = 1 fps, flame size = 512 × 512 pixels) and high- (scanning speed = 30 fps, flame size = 512 × 512 pixels) speed-modes of scanning were selected for observation. Under each condition of analysis, C_{per} was 8.8 × 10^{-5}.

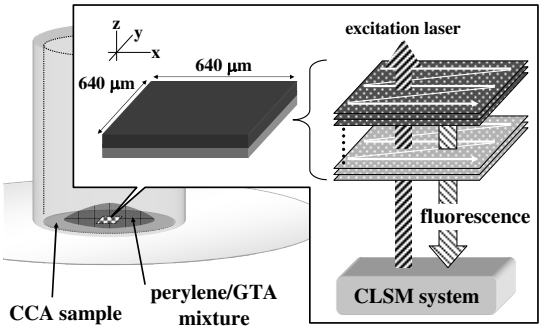

Fig. 5. Observation of perylene/GTA mixture in CCA sample by CLSM.

Figure 6 shows the chemical images of X-Y surface at 0, 2, 4, 6 and 8 μm-depth of CCA sample treated with perylene/GTA mixture under the CLSM conditions of low-speed-mode, ± 10 μm range and 1 μm intervals. Considering the influence of asperity on the air-contact surface of CCA sample, approximately 4.0×10^4 square μm of area of X-Y surface was selected from the observed areas for analysis. The blue color derived from the fluorescent intensity of perylene/GTA mixture was detected at 60 min at each depth of CCA sample. It was clear that the higher the depth of the film, the darker the blue color induced by sorbed perylene.

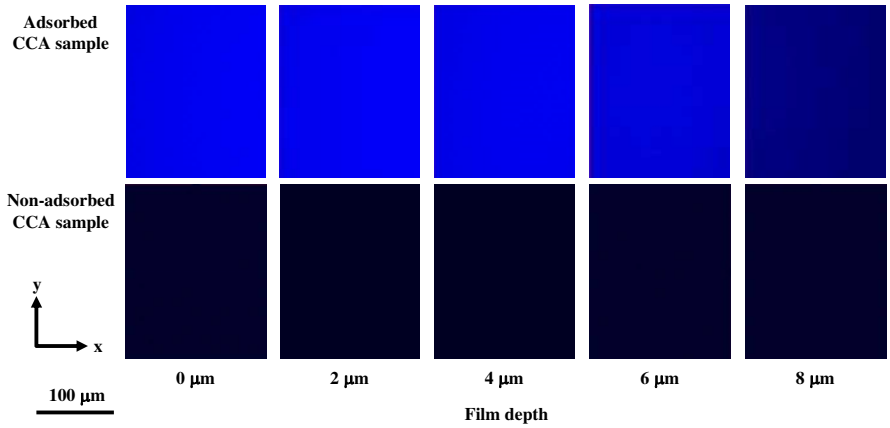

Fig. 6. Chemical images of X-Y surface at several depths of CCA sample at 60 min after the addition of perylene/GTA mixture obtained under conditions of low-speed-mode, ± 10 μm range and 1 μm intervals.

Figures 7-9 show changes in fluorescent intensities at each depth of the CCA sample. The intensity was calculated as an average of each pixel in a given analytical area. Three replicates of CLSM analysis of perylene (± SD) were performed for this study. In the horizontal axis, the 0 μm-depth represents the air-contact surface of the CCA sample. The results of sorbed perylene at the low-speed-mode, in the range of ± 10 μm and 1 μm intervals are shown in Figure 7, while the results of sorbed perylene at the low-speed-mode, in the range of ± 30 μm and 3 μm intervals are shown in Figure 8. Under both CLSM

conditions, the perylene-induced intensity was detected within 9-μm depth of the CCA sample and became lower with film depth. The fluorescence phenomena revealed that after starting the diffusion of absorbed perylene on the air-contact surface of the CCA sample, perylene dynamically sorbed into inner CCA sample with time for 60 min. By considering that at a film depth of higher than 12 μm the perylene-induced intensity was not detected in Figure 8, the scan range of ± 10 μm along the Z-axis would be sufficient for monitoring the perylene sorption behavior in this study. In contrast, at a high-speed-mode of scanning in the range of ± 10 μm (Figure 9), the increase in intensity of sorbed perylene was detected within almost the same (9 μm) depth of the film as that in Figure 7. Thus, the scanning speed of high-speed-mode with a wide range along the Z-axis in a rapid-CLSM analysis in seconds could be useful for dynamic and rapid observation of penetrant distribution in CCA sample. To evaluate the effect of optical path length on fluorescent intensity induced by perylene, 12 μl of perylene/ GTA mixture was analyzed as mentioned above with the use of a film-

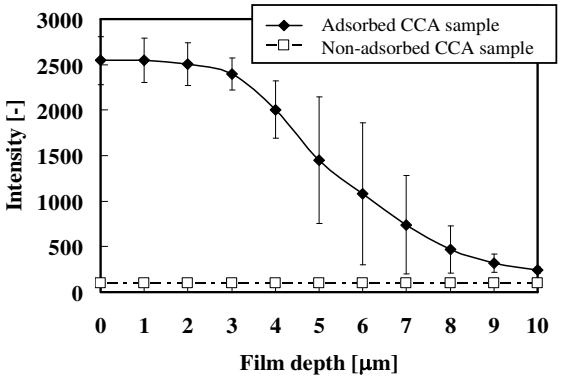

Fig. 7. Relationship between the depth of CCA sample and fluorescent intensity derived from perylene/GTA mixture obtained under conditions of low-speed-mode, ± 10 μm range and 1 μm intervals.

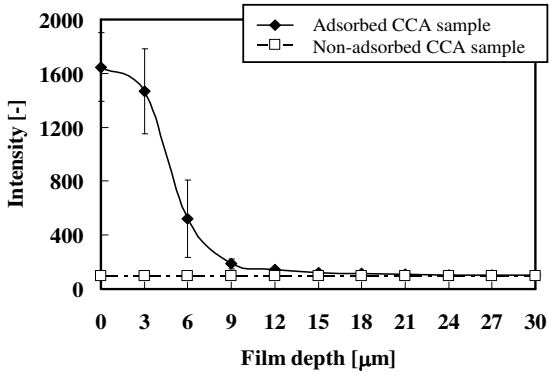

Fig. 8. Relationship between the depth of CCA sample and fluorescent intensity derived from perylene/GTA mixture obtained under conditions of low-speed-mode, ± 30 μm range and 3 μm intervals.

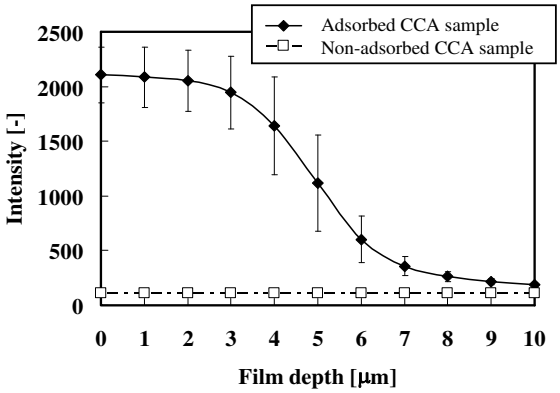

Fig. 9. Relationship between the depth of CCA sample and fluorescent intensity derived from perylene/GTA mixture obtained under conditions of high-speed-mode, ± 10 μm range and 1 μm intervals.

making-unit (without CA film). Figure 10 shows the relationship between the path length of CLSM and the fluorescent intensity of perylene. On the vertical axis, fluorescent intensity was calculated as an average of each pixel in the observation area at 1 min after pipetting the mixture onto the film-making-unit. On the horizontal axis, the value represents the distance from the top of the cover glass. As a result, the longer the distance, the lower the fluorescent intensity, suggesting that the power of the excitation laser or the intensity of the fluorescence would decay with the increase of optical path length. This result suggests that although the decay behavior of fluorescent intensity derived from perylene in the CCA sample was not clarified, the gradient of the amount of perylene must be sharper than gradients of the observed fluorescent intensities in Figures 7, 8 and 9.

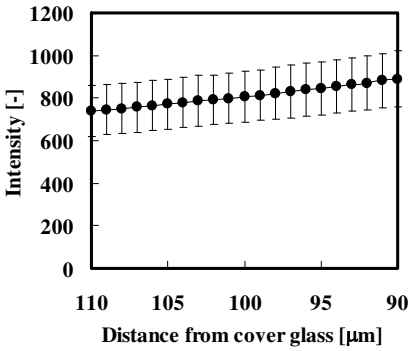

Fig. 10. Relationship between optical path length and fluorescent intensity derived from pelyrene/GTA mixture.

As to the sorption of compounds into polymer materials, physical and chemical parameters of compounds and/or polymers such as molar volume, solubility parameters, free energy and free volume determine the dynamics [11-13]. When taking particular note of the solubility parameter (SP), the affinity of a compound for polymer material is explained by two-dimensional distance (δ_c) defined as formula (2) [11],

$$\delta_c = \left[\left(\delta_{1np} - \delta_{2np} \right)^2 + \left(\delta_{1p} - \delta_{2p} \right)^2 \right]^{1/2} \quad (2)$$

where δ_t is the total SP value and δ_{np} and δ_p are nonpolar and polar components of δ_t, respectively, and the smaller the δ_c, the higher the affinity. Table 1 presents the SP values of CA, perylene and GTA, and the δ_c value of perylene and GTA from CA. The SP values of CA were as previously reported [36] and those of perylene and GTA were calculated using computational software, Molecular Modeling Pro (version 6.0.1, ChemSW, Inc., CA). The δ_c value of GTA was smaller than that of perylene and it was considered that the affinity of GTA for CA was higher than that of perylene. As a plasticizer for CA, GTA should accelerate the sorption of other compounds into polymer material, and it was thought that GTA had some effect on the sorption behavior of perylene into the CCA sample obtained in this study [10]. Therefore, in other words, this CLSM methodology can explain the sorption behavior of liquid additives such as GTA using the fluorescent reagent like perylene.

Compounds	SP [MPa$^{1/2}$]			δ_c* [MPa$^{1/2}$]
	δ_t	δ_{np}	δ_p	
CA	**25.1**	**21.6**	**12.7**	**-**
perylene	**26.0**	**26.0**	**1.3**	**12.2**
GTA	**27.2**	**26.3**	**6.8**	**7.6**

* Distance to CA

Table 1. Solubility parameter (SP) value and two-dimensional distance of compounds.

2.3 Calculation of diffusion coefficient of fluorescent reagent

Figure 11 shows change of fluorescent intensity of perylene in each depth of CCA sample measured by a CLSM system every 3 minutes to 30 minutes after dropping a 4 μl-perylene/additive mixture onto CCA sample. CLSM conditions were low-speed-mode and 1 μm intervals. On the horizontal axis, the 0 μm-depth indicates the air-contact surface of CCA sample. Fluorescent intensities in each depth were standardized by subtracting CCA-based intensity and subsequently dividing the obtained intensity by that of 0 μm-depth each time. As a result, the fluorescent intensity derived from perylene became higher in each depth over the course of time.

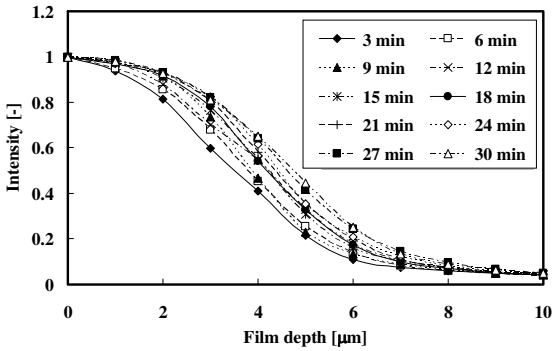

Fig. 11. Relationship between the depth of CCA sample and fluorescent intensity at several times after addition of perylene/GTA mixture.

From the results shown in Figure 11, the diffusion coefficient of perylene, D, was calculated based on Fick's second law given as formula (3),

$$\frac{\partial C}{\partial t} = D\frac{\partial}{\partial x}\left(\frac{\partial C}{\partial x}\right) \tag{3}$$

where C is a concentration of perylene, t is the time after the addition of mixtures and x is the film depth. The left side of the equation was obtained as the slope of standardized intensity, S_i, versus t in each depth of film because the intensity had a good linearity for the molar ratio of perylene (Figure 4). Then, the second term of the right side was calculated as the slope of a change of standardized intensity in 2 μm-depth range, $\partial S_i/\partial x$, versus x. Finally, D was calculated as the coefficient of both sides of the equation for each depth of film and was averaged. Considering a good agreement with Fick's second law, the calculation was performed in a particular film depth range where both S_i to t and $\partial S_i/\partial x$ to x relations had linearity. As shown in Figures 12 and 13, high linearity ($r > 0.969$) was obtained in each mixture and D was calculated in the range of 3 to 8 μm-depth of CCA sample and the value was 1.7×10^{-15} m²/s when mixed with GTA and added on CCA sample.

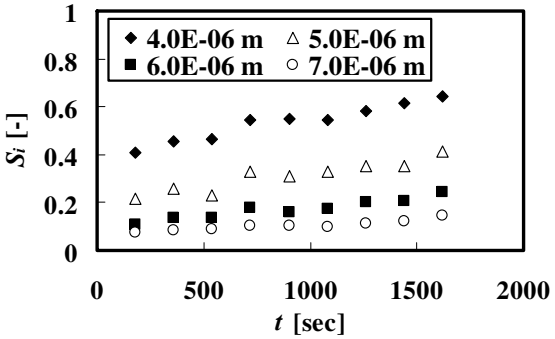

Fig. 12. Relationship between time after mixtures addition and standardized intensity.

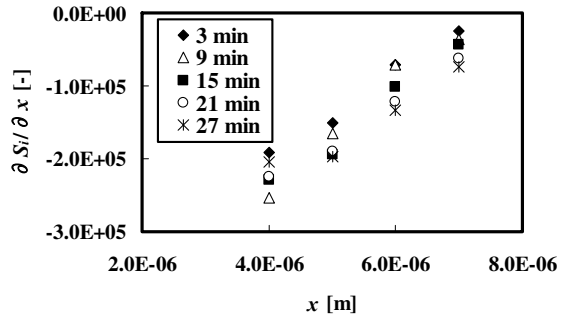

Fig. 13. Relationship between film depth and change of standardized intensity.

In this section, we visualized the dynamic distribution of perylene in CA film by applying a CLSM system for the first time. Analytical conditions of CLSM such as the scanning range

along the Z-axis and the scanning speed did not affect the results and diffusion coefficient of perylene in CCA sample was obtained according to Fick's second law. This methodology has an enormous advantage for evaluating the sorption behavior of penetrant into polymer; the proposed non-destructive confocal optics system enables direct cross-sectional analysis to be performed without any destruction of sorbed film.

3. Effect of additives on sorption behavior of fluorescent reagent

3.1 Difference of diffusion coefficient

As additives mixed with perylene and added to CCA sample, TEGDA (Mw = 234.3 g/mol, Tokyo Chemical Industry Co., Ltd., Tokyo, Japan), BGDA (Mw = 174.2 g/mol, Daicel Chemical Industries Ltd.), paraffin liquid (C ~ 28, Mw ~ 395 g/mol, Nacalai Tesque, Inc., Kyoto, Japan) and PEG (C ~ 4, Mw ~ 200 g/mol, Wako Pure Chemical Industries Ltd.) were used further to GTA. Each perylene/additive mixture was prepared at room temperature by dissolving perylene with an additive to achieve a desired molar ratio in the range of 2.1 to 13 × 10^{-5} of perylene defined as formula (4).

$$Molar\ ratio[-] = \frac{Perylene\ amount\ [mol]}{Perylene\ amount\ [mol] + Additive\ amount\ [mol]} \tag{4}$$

Fluorescent spectra of perylene/additive mixtures, additives and CCA sample when excited by diode laser at 408 nm are shown in Figure 14. The spectra clearly demonstrated that perylene/additive mixtures showed significant perylene-induced fluorescent intensity at around 470 and 503 nm, while no fluorescent intensities were observed for additives and CCA sample. This proves that any interference in fluorescence from additives or CA film could be excluded for an *in situ* penetration monitoring of perylene in CCA sample. Figure 15 shows the relationships between molar ratio of perylene in perylene/additive mixtures and fluorescent intensities. As a result, a good linearity (r > 0.978) was observed in each mixture in the range of 2.1 to 13 × 10^{-5} molar ratio of perylene.

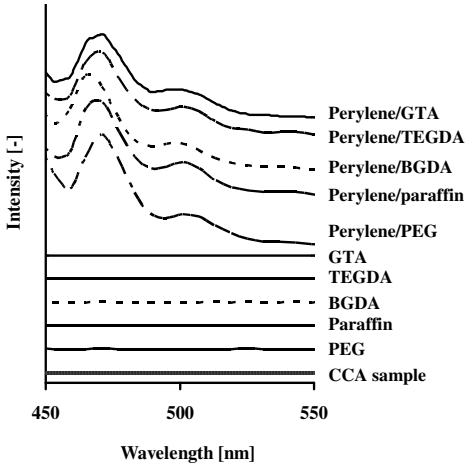

Fig. 14. Fluorescent spectra of perylene/additive mixtures, additives and CCA sample.

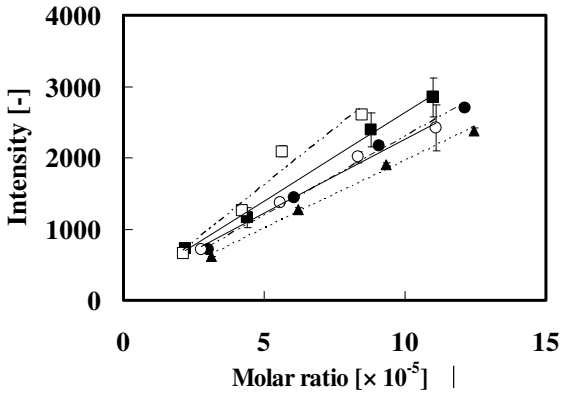

Fig. 15. Relationships between molar ratio and fluorescent intensity of perylene mixed with additives: GTA (■), TEGDA (●), BGDA (○), paraffin liquid (□) and PEG (▲).

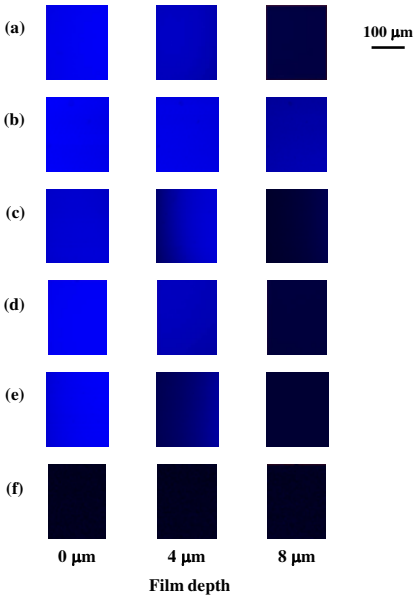

Fig. 16. Chemical images of CCA sample at several depths 9 minutes after addition of perylene/additive mixtures: (a) /GTA, (b) /TEGDA, (c) /BGDA, (d) /paraffin liquid, (e) /PEG and (f) control (without addition).

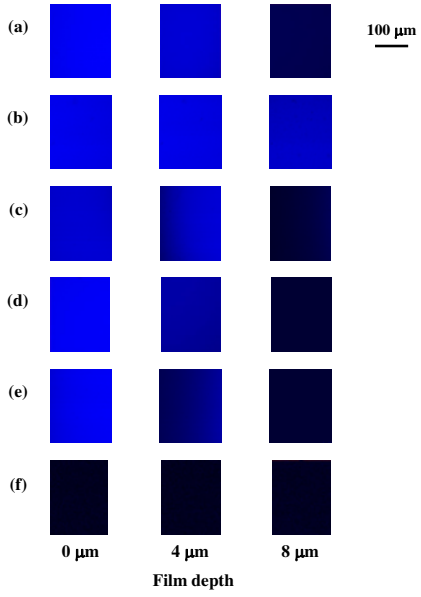

Fig. 17. Chemical images of CCA sample at several depths 21 minutes after addition of perylene/additive mixtures: (a) /GTA, (b) /TEGDA, (c) /BGDA, (d) /paraffin liquid, (e) /PEG and (f) control (without addition).

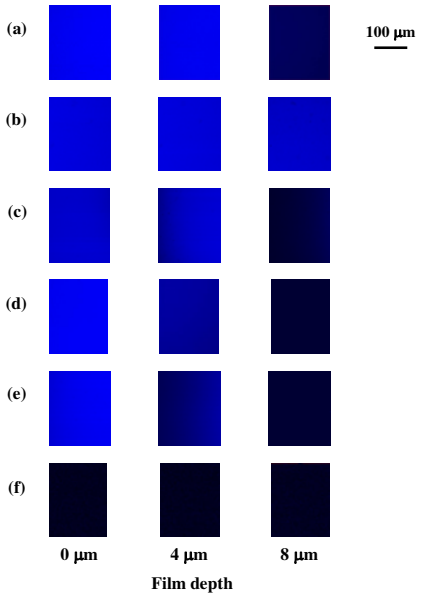

Fig. 18. Chemical images of CCA sample at several depths 30 minutes after addition of perylene/additive mixtures: (a) /GTA, (b) /TEGDA, (c) /BGDA, (d) /paraffin liquid, (e) /PEG and (f) control (without addition).

Change in fluorescent intensity of perylene in CCA sample during sorption experiments at room temperature was measured by a CLSM system every 3 minutes to 30 minutes after dropping a 4 μl-perylene/additive mixture (molar ratio of perylene was $8.8 \pm 0.5 \times 10^{-5}$) onto CCA sample. Chemical images at 0, 4 and 8 μm-depth of CCA sample treated with perylene/additive mixtures 3 minutes after the addition onto the film are shown in Figure 16 as well as the time-course images obtained at 21 and 30 minutes after the addition (in Figures 17 and 18, respectively). CLSM conditions were identical with the aforementioned section 2 except that speed-mode was low and the intervals were 1 μm. Considering the influence of asperity on air-contact surface of CCA sample, approximately 4.0×10^4 square μm of areas were selected from the observation areas for analysis. The blue color derived from the fluorescent intensity of perylene was detected in each image. It was clear that the higher the depth of the film, the darker the blue color induced by sorbed perylene. The results in Figures 16, 17 and 18 prove that the brightness of blue color became higher over time after the mixture addition, especially for GTA, TEGDA and BGDA. These results indicate that the sorption of perylene/additive mixture progressively proceeded from the top of CCA sample to inside of the film. The brightness and its change were the highest for perylene/TEGDA mixture.

To quantify these behaviors, fluorescent intensities were calculated as an average of each pixel in a given analytical area for perylene/additive mixture. Figure 19 shows changes of relationships between the film depth and the standardized intensities, in which the intensity was averaged through three replicates of CLSM analysis. As a result, the change in intensity over time was the largest in perylene/TEGDA mixture. In particular, the standardized intensity in perylene/TEGDA mixture increased by a factor of 0.37 at 8 μm-depth from 3 to 30 minutes after the addition of mixture. Perylene-induced intensities also increased clearly

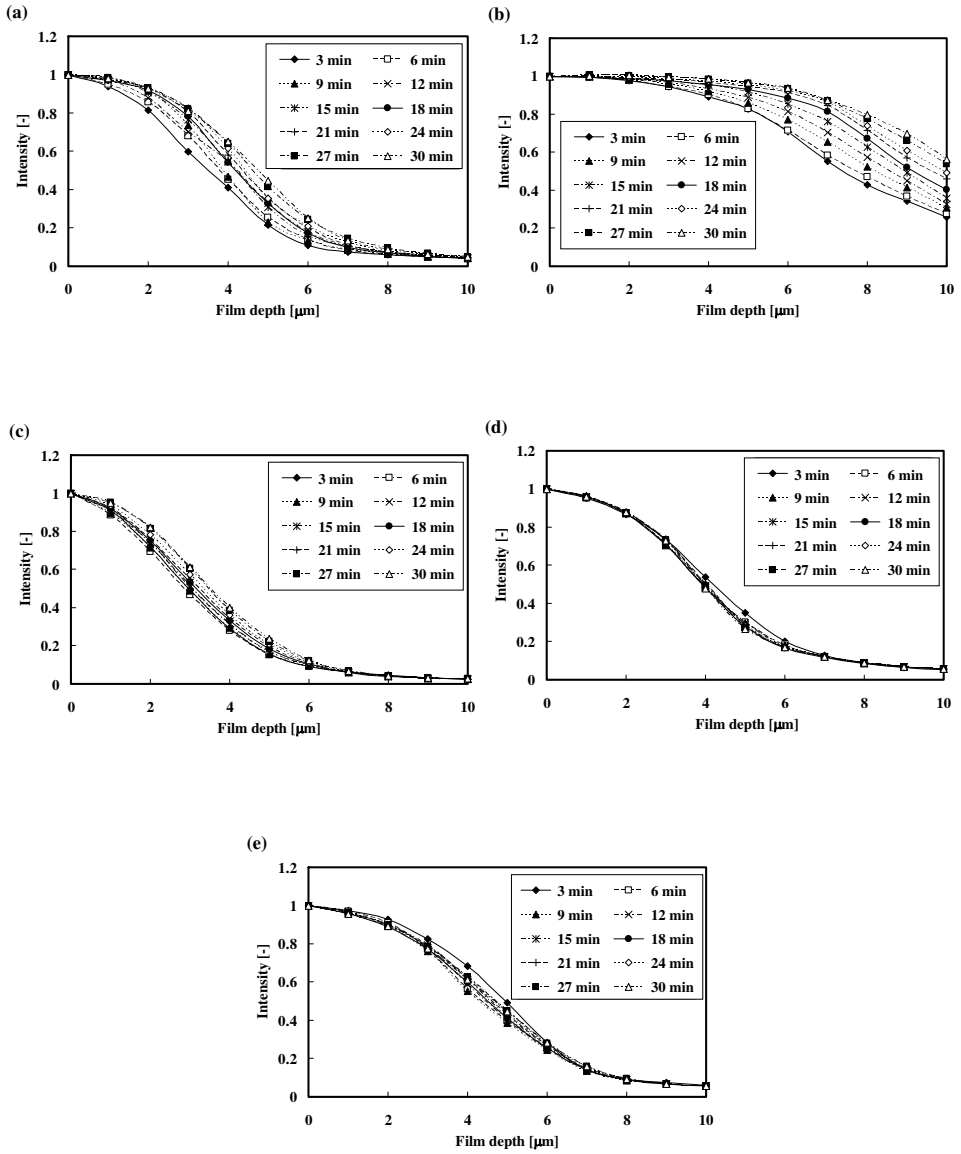

Fig. 19. Relationship between the depth of CCA sample and fluorescent intensity at several times after addition of perylene/additive mixtures: (a) /GTA, (b) /TEGDA, (c) /BGDA, (d) /paraffin liquid and (e) /PEG.

when mixed with GTA and BGDA, and their increment was a factor of 0.24 at 4 μm-depth and 0.12 at 3 μm-depth, respectively. For paraffin liquid and PEG, on the other hand, changes in intensities were as little as 0.01 at any film depth, though the intensities were detected within almost 9-μm depth of CCA sample.

From the results shown in Figure 19, the diffusion coefficient of perylene, *D*, was calculated based on Fick's second law as mentioned in section 2. Figure 20 shows the *D* values of perylene in CCA sample when mixed with additives. The value varied depending on the additives and became the highest in the mixture with TEGDA (8.9×10^{-15} m²/s). The order was TEGDA > GTA (1.7×10^{-15} m²/s) > BGDA (1.3×10^{-15} m²/s) > PEG (0.54×10^{-15} m²/s) > paraffin liquid (0.34×10^{-15} m²/s) in descending order, indicating that the additives greatly affected the diffusion behavior of perylene in CCA sample.

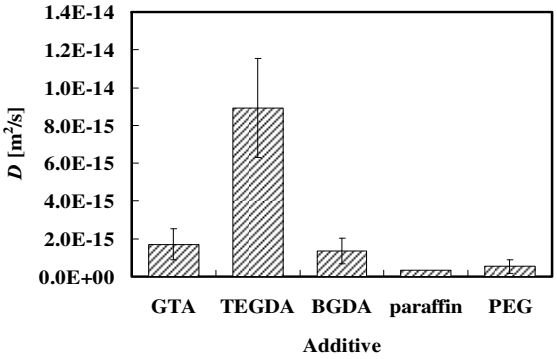

Fig. 20. Diffusion coefficient of perylene mixed with additives in CCA sample. Data are the mean ± SD (n = 3).

3.2 Effect of physicochemical properties of additives

The above *D* values suggest that the sorption behavior of perylene in CCA sample was largely affected by the physicochemical properties of additives. Table 2 displays SP values of perylene, additives and CA. SP values of TEGDA, BGDA, paraffin liquid and PEG were calculated using with Molecular Modeling Pro. δ_c values of additives from perylene and CA were calculated with the formula (2), and Figure 21 shows an index of chemical affinities, $1/\delta_c$. The chemical affinities of additives with perylene or CA would affect the perylene-additive compatibility or sorption of the additive itself into CCA sample.

Compound	SP [MPa$^{1/2}$]		
	δ_t	δ_{np}	δ_p
perylene	26.0	26.0	1.3
GTA	27.2	26.3	6.8
TEGDA	25.9	25.3	5.7
BGDA	18.9	18.4	4.1
paraffin	16.7	16.7	0
PEG	22.5	22.0	4.5
CA	25.1	21.6	12.7

Table 2. SP value of compounds.

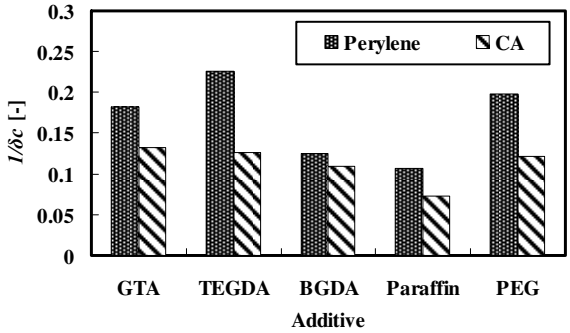

Fig. 21. Chemical affinity of additives with perylene and CA.

It was considered that the highest D value in perylene/TEGDA mixture was due to the high affinity of perylene with TEGDA. In contrast, the lowest D value in perylene/paraffin liquid mixture was caused by the low affinity of perylene with both paraffin liquid and CCA sample. For GTA, BGDA and PEG, difference of D could not be explained only by chemical affinities. Although the $1/\delta_c$ values from CA were almost the same, the $1/\delta_c$ values from perylene were PEG > GTA > BGDA in descending order. This order did not agree with that of D shown in Figure 20; namely, the diffusion coefficient of perylene in CCA sample added with PEG was lower than the expected value.

Physical parameters such as the molecular size and viscosity of chemicals were then taken into consideration as external affecting factors. When considering the sorption of additives into CA film, the diffusion coefficient of additive, D', may be influenced by its molecular diameter, d, and viscosity, η. The relationships of those parameters are given by Stokes-Einstein equation as follows:

$$D' = \frac{kT}{3\pi d\eta} \tag{5}$$

where k and T are Boltzmann's constant and absolute temperature, respectively. Table 3 presents the sphere-equivalent molecular diameter and viscosity of additives. Sphere-equivalent molecular diameters were calculated by Molecular Modeling Pro. And viscosities were measured at 25 °C by digital viscometer (DVL-BII, Toki Sangyo Co., Ltd., Tokyo, Japan). As a result, the diffusion coefficient of PEG in CA film was calculated to be lower than those of GTA and BGDA on account of the higher viscosity of PEG. Thus, the lower D of perylene in PEG (Figure 20) would be caused by the poor diffusion of PEG itself in CCA sample. For perylene/paraffin liquid mixture, it was thought that the lowest D of perylene was due not only to low chemical effects but also to the physical properties of paraffin liquid such as high molecular size and high viscosity.

In this section, the effects of various additives, GTA, TEGDA, BGDA, paraffin liquid and PEG, on the sorption behavior of perylene into CCA sample were compared. The sorption behavior of perylene was visualized dynamically by CLSM methodology while diffusion coefficients were calculated according to Fick's second law. Taking these findings together, it was confirmed that the diffusion coefficient of perylene was influenced by both chemical affinities for additives or CCA sample and the diffusivity of additive in CCA sample. The highest diffusion coefficient of perylene, 8.9×10^{-15} m^2/s, obtained in TEGDA mixture was

due to the high chemical affinity of TEGDA with perylene ($1/\delta_c$ value was 0.23). Meanwhile, in the case of perylene/GTA, BGDA or PEG mixture, the difference in diffusion coefficient of perylene (1.7×10^{-15}, 1.3×10^{-15} and 0.54×10^{-15} m^2/s, respectively) could not be explained only by the chemical affinities between additives and perylene ($1/\delta_c$ values were 0.18, 0.12 and 0.20, respectively). Based on physical parameters, it was suggested that the lower diffusion coefficient of perylene with PEG into CCA sample would be attributed to the high viscosity of PEG. The lowest diffusion coefficient of perylene, 0.34×10^{-15} m^2/s, when mixed with paraffin liquid, would be caused by both the low chemical affinity and the low diffusivity of paraffin liquid in CCA sample.

Additive	Molecular diameter d [nm]	Viscosity η [cPs]
GTA	**0.73**	**17.0**
TEGDA	**0.71**	**9.8**
BGDA	**0.64**	**3.2**
paraffin	**0.96**	**147.5**
PEG	**0.71**	**48.8**

Table 3. Molecular diameter and viscosity of additives.

4. Effect of film types and film depth on sorption behavior of fluorescent reagent

4.1 Difference of diffusion coefficient caused by multiple stratification treatment of film

As a different type of CA film from CCA sample, open-system CA film (OCA) was prepared by putting an aliquot (4 ml) of CA solution (2.0 w/v % in acetone) into glass petri dish (27 mmϕ), vaporizing excess acetone for 7 days at room temperature. After drying *in vacuo* overnight, film was peeled off from petri dish and fixed between two neodymium magnets (Figure 22, 23 mmϕ of inner diameter and 1 mm thick). The prepared OCA sample was 60 ± 10 μm thick.

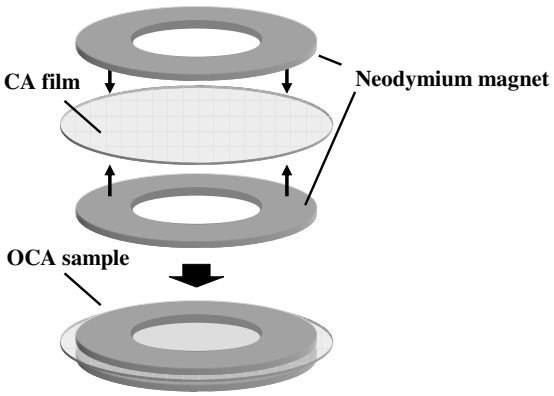

Fig. 22. OCA sample fixed between neodymium magnets.

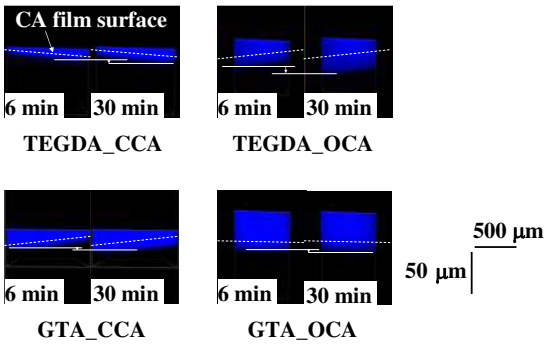

Fig. 23. Time-course cross-sectional chemical images (X-Z surface) of CCA and OCA samples.

Perylene/GTA or perylene/TEGDA mixtures were added on the CCA or OCA sample and the sorption behavior of perylene in films were observed by the CLSM methodology. CLSM conditions were identical with the aforementioned section 3 except that analytical depth from the air-contact surface of film samples was 20 μm with intervals of 1 μm. The molar ratio, defined by formula (3), in each perylene/GTA and perylene/TEGDA mixture was 9.1×10^{-5} and 8.8×10^{-5}, respectively.

Three-dimensional chemical images of CA film samples treated with perylene/additive mixtures were reconstructed by the chemical images of X-Y surface obtained at several depths of film samples. Figure 23 shows cross-sectional chemical images (X-Z surface) of CCA and OCA samples at 6 and 30 minutes after the addition of perylene/additive mixtures. Although there are some influences of asperity or slant on air-contact surface of film samples, the blue color derived from the fluorescent intensity of perylene was detected in each image. It was clear that the blue color expanded to deeper area over time after the addition of mixtures in each CA film sample. These results describe that the sorption of perylene/additive mixture proceeded progressively from the top of film samples to inside of the film. With respect to the effect of the additives on the perylene-sorption, the change was higher for perylene/TEGDA mixture in both CCA and OCA samples. Intriguingly, perylene-sorption behavior in the OCA sample became more intense than that in the CCA sample especially for perylene/TEGDA mixture.

To quantify this behavior, fluorescent intensities derived from perylene in CA film samples were calculated as an average of each pixel in X-Y surfaces. Approximately 4.0×10^4 square μm of areas were selected from the observation areas for analysis. Figures 24-27 illustrate variations of intensities in each depth of CA film samples, in which the intensity was averaged through three replicates. On the horizontal axis, the 0 μm-depth indicates the air-contact surface of film samples. Fluorescent intensities in each depth were standardized by subtracting CA-based intensity and subsequently dividing the obtained intensity by that of 0 μm-depth each time.

Consequently, the standardized intensity (I_s) of each depth increased progressively from 6 to 30 minutes after adding mixtures. Concerning the CCA samples (Figures 24 and 25), I_s increased by a factor of 0.34 at 8 μm-depth and 0.22 at 4 μm-depth in perylene/TEGDA and perylene/GTA mixtures, respectively. For the OCA samples (Figures 26 and 27), on the

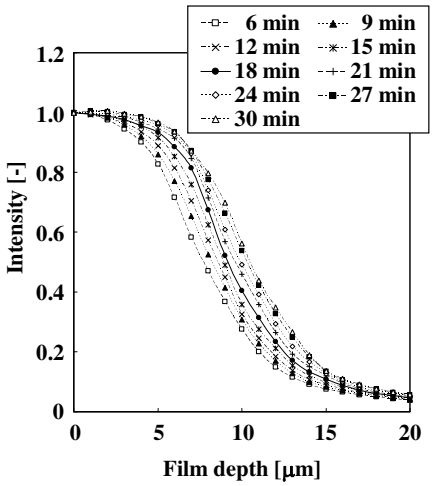

Fig. 24. Relationship between the depth of CCA sample and I_s at several times after addition of perylene/TEGDA mixture.

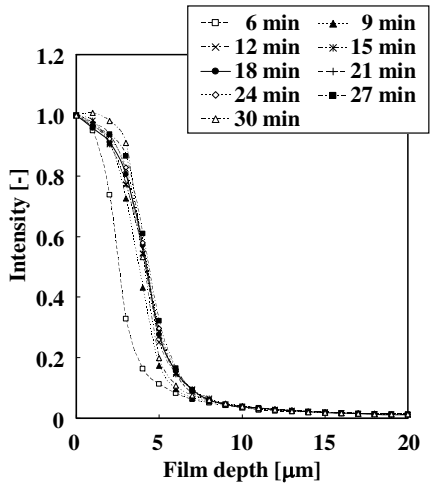

Fig. 25. Relationship between the depth of CCA sample and I_s at several times after addition of perylene/GTA mixture.

other hand, each increment was a factor of 0.26 at 14 μm-depth and 0.20 at 9 μm-depth in perylene/TEGDA and perylene/GTA mixtures, respectively. From the results illustrated in Figures 24-27, the diffusion coefficient of perylene, D, was calculated in the same way as described in section 2. Figure 28 displays the D values of perylene in CCA and OCA film samples when mixed with additives. Concerning the CCA samples, D values were calculated in 10 to 13 and 3 to 8 μm-depth range in perylene/TEGDA and perylene/GTA mixtures, respectively. For the OCA samples, D values were calculated in 14 to 17 and 9 to 11 μm-depth range in perylene/TEGDA and perylene/GTA mixtures, respectively. It was

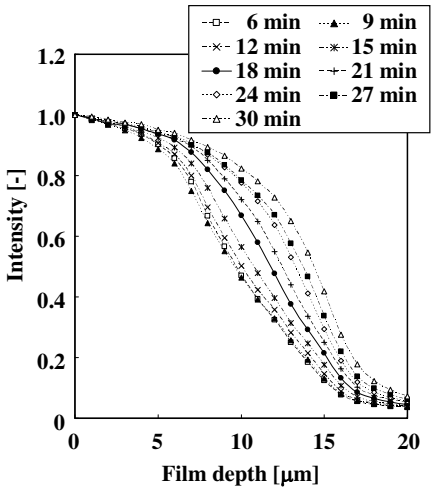

Fig. 26. Relationship between the depth of OCA sample and I_s at several times after addition of perylene/TEGDA mixture.

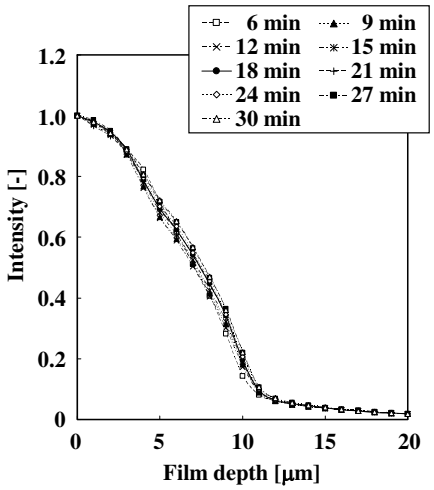

Fig. 27. Relationship between the depth of OCA sample and I_s at several times after addition of perylene/GTA mixture.

confirmed that D value varied depending on the kind of additives and the CA film type. In both cases of CCA and OCA samples, D values of perylene when mixed with TEGDA (CCA: $8.9 \pm 2.6 \times 10^{-15}$ m²/s, OCA: $11 \pm 5.1 \times 10^{-15}$ m²/s) were higher than those of GTA (CCA: $1.7 \pm 0.83 \times 10^{-15}$ m²/s, OCA: $3.3 \pm 2.2 \times 10^{-15}$ m²/s). And it was found that regardless of the kind of additives, D values of perylene in CA film became higher for the OCA samples (TEGDA: $11 \pm 5.1 \times 10^{-15}$ m²/s, GTA: $3.3 \pm 2.2 \times 10^{-15}$ m²/s) than for the CCA samples (TEGDA: $8.9 \pm 2.6 \times 10^{-15}$ m²/s, GTA: $1.7 \pm 0.83 \times 10^{-15}$ m²/s).

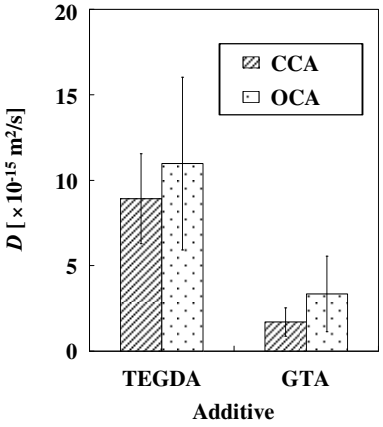

Fig. 28. Diffusion coefficients of perylene in CCA and OCA samples when mixed with TEGDA or GTA. Data are the mean ± SD (n = 3).

As described in section 3, diffusion coefficient of perylene in CCA sample was affected by physicochemical properties of additives, and regarding the higher D value of perylene mixed with TEGDA (8.9×10^{-15} m^2/s) than that of mixed with GTA (1.7×10^{-15} m^2/s), it was attributed to higher chemical affinity of perylene with TEGDA based on estimation with solubility parameters (SPs). Similarly in the case of OCA sample, as the above results in this study suggested, the order of the D value of perylene, TEGDA mixture (11×10^{-15} m^2/s) > GTA mixture (3.3×10^{-15} m^2/s), was attributed to the difference of chemical affinity of perylene with additives.

Regardless of the kind of additives, D values of perylene in OCA samples were higher than those of in CCA samples. Figure 29 represents shifts of I_s in each depth of CCA and OCA samples 1, 2 and 24 hours after the addition of perylene/TEGDA mixture. With the exception that cross-sectional region for scanning was 0-40 μm-depth from air-contact surface of film samples, experimental conditions and analytical protocols were same as mentioned above. As for the CCA sample, no investigation was carried out on a progressive sorption of perylene into the film but on a swing-over of perylene-sorption to some extent after 1 hour. I_s at 1, 2 and 24 hours after the addition of perylene/TEGDA mixture were 0.015, 0.014 and 0.012 at 20 μm-depth and 0.0034, 0.0035 and 0.0033 at 40 μm-depth, respectively. This result pointed out that perylene-sorption came to equilibrium around 1 hour after the addition of mixture, and the distribution ratio of perylene at 40 μm-depth was 0.3 % compared with the air-contact surface (0 μm-depth) of the film. For the OCA sample, on the other hand, it was identified that sorption of perylene into the film was progressing even at 24 hours after the addition of mixture. I_s at 1, 2 and 24 hours after the addition of perylene/TEGDA mixture were 0.30, 0.88 and 1.1 at 20 μm-depth and 0.017, 0.27 and 1.1 at 40 μm-depth, respectively. This result represented that perylene was homogeneously-distributed in OCA sample by 24 hours after the mixture addition as opposed to CCA sample.

Studies on gas permeation through polymer films revealed that the permeability of multilayer was not always correspondent to the multiplication of those of each consisting monolayer [37] or the permeability of multilayer differed depending on the side of coating layer (inside or outside) [38]. Considering the cover glass of the CCA sample as a coating layer

of CA film, the above results clarified that diffusion coefficient and distribution of perylene in CA film largely vary with multiple stratification treatment.

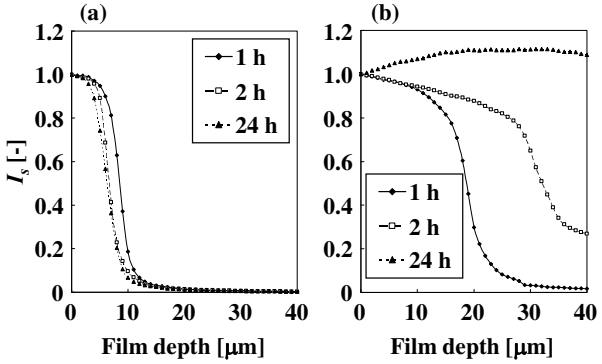

Fig. 29. Relationship between the depth of CA film and I_s at several times after addition of perylene/TEGDA mixture: (a) CCA and (b) OCA.

4.2 Film depth dependence of diffusion coefficient

To promote more understandings for sorption behavior of perylene into CA film, diffusion coefficients at each film depth were calculated pursuant to Fick's second law. Figure 30 describes relationships between film depth and diffusion coefficient of perylene in CCA and OCA samples. Greatly interesting to note, these results pointed out clearly that there were strong negative correlations between the two, *i.e.* the deeper the film depth, the lower the diffusivity of perylene regardless of type of additives and films. As is well known, Fick's second law is based on hypothesis that although concentration gradient penetrating to film depth transforms over the time of course, rate of its transformation is constant and D is obtained as a constant number. These results, however, contradicted the hypothesis. Comparing the slopes obtained approximate linearization, absolute values of OCA samples (TEGDA: 3.9×10^{-15}, GTA: 2.2×10^{-15}) were higher than those of CCA samples (TEGDA: 2.0×10^{-15}, GTA: 0.64×10^{-15}). It means that influence of film depth increase on decline of diffusivity was larger for OCA samples than for CCA samples.

As factors causing the film depth dependence of diffusion coefficient, two viewpoints were considered. The first factor was the effect of additives mixed with perylene. With respect to the diffusion of penetrant in polymer materials, free volume theory was proposed in 1960s [39] and recently, it has been generally thought that amorphous portion in polymer material is dominating diffusion pathway [40-46]. It was considered that with the diffusion of TEGDA or GTA, amorphous portion, *i.e.* diffusion pathway for perylene, gradually increased on account of CA solubility [33] of additives. As a result, D value of perylene in superficial part of CA film was higher than that of deep part. The second factor was the concentration dependence of diffusion coefficient. It has been reported that the higher the concentration of penetrant in experimental system, the higher the diffusion coefficient of penetrant in the polymer materials [47, 48]. In polymer materials, the concentration of penetrant should be different in accordance with the distance from liquid/solid or vapor/solid boundaries. It was considered that the aforementioned film depth dependence of D value directly indicates the concentration

dependence of diffusion coefficient in the CA film. As for the CCA sample, perylene had a lower D value than that obtained above (3.8×10^{-15} m^2/s < 8.9×10^{-15} m^2/s) when mixed with TEGDA at lower molar ratio ($0.28 \times 10^{-5} < 9.1 \times 10^{-5}$). Moreover, this result proves that the diffusion coefficient of perylene had the concentration dependence.

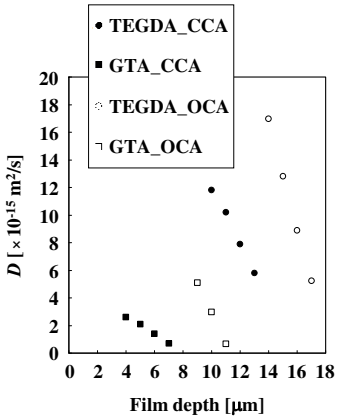

Fig. 30. Relationship between CA film depth and diffusion coefficient of perylene.

In this section, the effects of kinds of additives, TEGDA and GTA, and film types, CCA and OCA, on the sorption behavior of perylene into CA film were evaluated. Through dynamic monitoring of the perylene-penetration by CLSM methodology, overall diffusion coefficients of perylene in CA film as well as its film depth dependence were calculated according to Fick's second law to be assessed.

Higher chemical affinity of TEGDA with perylene than that of GTA commonly caused the higher diffusion coefficient of perylene both for CCA sample (TEGDA: 8.9×10^{-15} m^2/s > GTA: 1.7×10^{-15} m^2/s) and OCA sample (TEGDA: 11×10^{-15} m^2/s > GTA: 3.3×10^{-15} m^2/s). What is really interesting was that perylene had higher diffusivity in OCA sample than CCA sample beyond types of additives. In conclusion, it was simultaneously clarified that when mixed with TEGDA, perylene appeared homogeneously-distributed in OCA sample by 24 hours after the mixture addition (I_s = 1.1 at 40 μm-depth of CA film) as opposed to CCA sample (I_s = 0.0033 same as above). These results demonstrated that diffusion coefficient and distribution of perylene in CA film largely vary with multiple stratification treatment.

From the results on the film depth dependence of diffusion coefficient, greatly interesting to note, it was explained clearly that the deeper the film depth, the lower the diffusivity of perylene regardless of type of additives and films. Although this finding contradicted the hypothesis of Fick's second law, gradual increase in diffusion pathway for perylene caused by additive diffusion as well as concentration dependence of perylene's diffusion coefficient were considered as factors.

5. Conclusions

In this chapter, the application of CLSM technique was described to observe the fluorescent reagent sorption behavior into polymer material in real-time and non-destructively. In section 2, the dynamic distribution of perylene into CA film (CCA sample) was visualized for the first

time, and the analytical conditions of CLSM such as the scanning range along the Z-axis and the scanning speed did not affect the results. In section 3, the effects of various additives, GTA, TEGDA, BGDA, paraffin liquid and PEG, on the sorption kinetics of perylene into CCA sample were compared by calculating diffusion coefficients of perylene according to Fick's second law. As a result, it was revealed that the diffusion coefficient of perylene was influenced by not only chemical affinities for additives or CCA sample and the diffusivity of additive in CCA sample but also by physical parameters such as molecular size or viscosity of additives. In section 4, effects of film types and film depth on diffusion coefficient of fluorescent reagent were examined as a further development of CLSM methodology. It was directly clarified that diffusion coefficient and distribution of perylene in CA film were declined with multiple stratification treatment. Thus, the deeper the film depth, the lower the diffusivity of perylene regardless of type of additives and films caused by additives diffusion into the film as well as concentration dependence of perylene's diffusion coefficient.

The aforementioned results and findings could be directly achieved owing to the advantages of CLSM system, that is, real-time and non-destructive visualization method for sorption dynamics. It was proved that our proposed CLSM methodology should be beneficial to promote better understandings for sorption behavior in the field of material science and engineering industries.

6. Acknowledgment

This study was conducted with the technical support of Nikon Instech Co., Ltd., Tokyo, Japan. We are grateful to Mr. Toyofumi Kameoka and Ms. Takayo Furuya for their operational support of the CLSM system.

7. References

[1] Hofmann, G. H.; Lee, W. C. J. Vinyl Add. Tech., 2006, 12, 33.
[2] Deanin, R. D.; Shah, N. A. J. Vinyl Tech., 1983, 5, 167.
[3] Ware, R. A.; Tirtowidjojo, S; Cohen, C. J. Appl. Polym. Sci., 1981, 26, 2975.
[4] Bouajila, J.; Dole, P.; Joly, C.; Limare, A. J. Appl. Polym. Sci., 2006, 102, 1445.
[5] Sakata, I.; Senju, R. J. Appl. Polym. Sci., 1975, 19, 2799.
[6] Shimoda, M.; Nitanda, T.; Kadota, N.; Ohta, H.; Suetsuna, K.; Osajima, Y. J. Jpn. Soc. Food Sci. Technol., 1984, 31, 697.
[7] Leufven, A.; Hermansson, C. J. Sci. Food Agric., 1994, 64, 101.
[8] Sadler, G. D.; Braddock, R. J. J. Food Sci., 1991, 56, 35.
[9] Kalachandra, S.; Turner, D. T. J. Polym. Sci.: Part B: Polym. Phys., 1987, 25, 697.
[10] Kalaouzis, P. J.; Demertzis, P. G.; Kontominas, M. G. Packag. Technol. Sci., 1993, 6, 261.
[11] Matsui, T.; Nagashima, K.; Fukamachi, M.; Shimoda, M.; Osajima, Y. J. Agric. Food Chem., 1992, 40, 1902.
[12] Matsui, T.; Fukamachi, M.; Shimoda, M.; Osajima, Y. J. Agric. Food Chem., 1994, 42, 2889.
[13] Fukamachi, M.; Matsui, T.; Shimoda, M.; Osajima, Y. J. Agric. Food Chem., 1994, 42, 2893.
[14] Shimoda, M.; Matsui, T.; Osajima, Y. J. Jpn. Soc. Food Sci. Technol., 1987, 34, 402.
[15] Matsui, T.; Shimoda, M.; Osajima, Y. J. Jpn. Soc. Food Sci. Technol., 1989, 36, 52.

[16] Hellsing, M.; Fokine, M.; Claesson, Å.; Nilsson, L. -E.; Margulis, W. Appl. Surf. Sci., 2003, 203-204, 648.
[17] Van Thienen, T. G.; Demeester, J.; De Smedt, S. C. Int. J. Pharm., 2008, 351, 174.
[18] Wu, L.; Brazel, C. S. Int. J. Pharm., 2008, 349, 144.
[19] Hubbuch, J.; Linden, T.; Knieps, E.; Ljunglöf, A.; Thömmes, J.; Kula, M. R. J. Chromatogr. A, 2003, 1021, 93.
[20] Hubbuch, J.; Linden, T.; Knieps, E.; Thömmes, J.; Kula, M. R. J. Chromatogr. A, 2003, 1021, 105.
[21] Yamaguchi, S. J. Kyorin Med. Soc., 2003, 34, 139.
[22] Wang, C.; Zhu, L.; Qiu, Y. J. Appl. Polym. Sci., 2008, 107, 1471.
[23] Wang, Y.; Yang, C.; Tomasko, D. Ind. Eng. Chem. Res., 2002, 41, 1780.
[24] Hasegawa, T.; Matsui, T.; Matsumoto, K. J. Appl. Polym. Sci., 2010, 116, 1552.
[25] Hasegawa, T.; Matsui, T.; Matsumoto, K. J. Appl. Polym. Sci., 2010, 116, 1710.
[26] Hasegawa, T.; Matsumoto, K.; Matsui, T. J. Appl. Polym. Sci., *in press*.
[27] Kutowy, O.; Thayer, W. L.; Tigner, J.; Sourirajan, S.; Dhawan, G. K. Ind. Eng. Chem. Prod. Res. Dev., 1981, 20, 354.
[28] Lance, S. K.; Stephen, G. W.; Kamal, Z. I. Anal. Chem., 1989, 61, 303.
[29] Perrin, L.; Nguyen, Q. T.; Sacco, D.; Lochon, P. Polym. Int., 1997, 42, 9.
[30] Roussis, P. P. Polymer, 1981, 22, 768.
[31] Roussis, P. P. Polymer, 1981, 22, 1058.
[32] Ohnishi, A.; Maeda, K.; Endo, Y.; Akinaga, Y.; Uehara, M. Senbai Chuken-ho, 1972, 114, 105.
[33] Maeda, K.; Anzai, Y.; Sawakuri, T.; Noguchi, K. Senbai Chuken-ho, 1975, 117, 109.
[34] Kawamoto, J. Jpn. Pat. 5,068,527 (A), 1993.
[35] Baggett, M. S.; Morie, G. P. Beitr. Tabakforsch., 1975, 8, 150.
[36] Burke, J. Book and Paper Group Annual, 1984, 3, 13.
[37] Mrkić, S.; Galić, K.; Ivanković, M.; Hamin, S.; Ciković, N. J. Appl. Polym. Sci., 2006, 99, 1590. 38. Alger, M. M.; Stanley, T. J.; Day, J. Polym. Eng. Sci., 1989, 29, 639.
[39] Fujita, H. Fortschr. Hochpolym. –Forsh., 1961, 3, 1.
[40] Olkhov, A. A.; Vlasov, S. V.; Iordanskii, A. L.; Zaikov, G. E.; Lobo, V. M. M. J. Appl. Polym. Sci., 2003, 90, 1471.
[41] Yasuda, H.; Peterlin, A. J. Appl. Polym. Sci., 1974, 18, 531.
[42] Michaels, A. S.; Bixler, H. J. J. Polym. Sci., 1961, 50, 393.
[43] Villaluenga, J. P. G.; Seoane, B.; Compañ, V. J. Appl. Polym. Sci., 1998, 70, 23.
[44] Compañ, V.; Andrio, A.; López, M. L.; Alvarez, C.; Riande, E. Macromolecules, 1997, 30, 3317.
[45] Wang, L. H.; Porter, R. S. J. Polym. Sci., 1984, 22, 1645.
[46] Nikishin, E. L.; Chalykh, E. A.; Avgonov, A.; Kulenznev, V. N.; Neverov, A. N. Colloid J., 1979, 40, 660.
[47] Vrentas, J. S.; Duda, J. L.; Ni, Y. C. J. Polym. Sci., Polym. Physics Ed., 1977, 15, 2039.
[48] Sano, Y.; Yamamoto, S. J. Chem. Eng. Jpn., 1990, 23, 331.

Laser Scanning, Theory and Applications

Edited by Prof. Chau-Chang Wang

ISBN 978-953-307-205-0
Hard cover, 566 pages
Publisher InTech
Published online 26, April, 2011
Published in print edition April, 2011

Ever since the invention of laser by Schawlow and Townes in 1958, various innovative ideas of laser-based applications emerge very year. At the same time, scientists and engineers keep on improving laser's power density, size, and cost which patch up the gap between theories and implementations. More importantly, our everyday life is changed and influenced by lasers even though we may not be fully aware of its existence. For example, it is there in cross-continent phone calls, price tag scanning in supermarkets, pointers in the classrooms, printers in the offices, accurate metal cutting in machine shops, etc. In this volume, we focus the recent developments related to laser scanning, a very powerful technique used in features detection and measurement. We invited researchers who do fundamental works in laser scanning theories or apply the principles of laser scanning to tackle problems encountered in medicine, geodesic survey, biology and archaeology. Twenty-eight chapters contributed by authors around the world to constitute this comprehensive book.

INTECH
open science | open minds

InTech Europe
University Campus STeP Ri
Slavka Krautzeka 83/A
51000 Rijeka, Croatia
Phone: +385 (51) 770 447
Fax: +385 (51) 686 166
www.intechopen.com

InTech China
Unit 405, Office Block, Hotel Equatorial Shanghai
No.65, Yan An Road (West), Shanghai, 200040, China
中国上海市延安西路65号上海国际贵都大饭店办公楼405单元
Phone: +86-21-62489820
Fax: +86-21-62489821